THE BELL SYSTEM
TECHNICAL JOURNAL
DEVOTED TO THE SCIENTIFIC AND ENGINEERING
ASPECTS OF ELECTRICAL COMMUNICATION

Volume 48 November 1969 Number 9

Coupled Wave Theory for Thick Hologram Gratings

By HERWIG KOGELNIK

(Manuscript received May 23, 1969)

A coupled wave analysis is given of the Bragg diffraction of light by thick hologram gratings, which is analogous to Phariseau's treatment of acoustic gratings and to the "dynamical" theory of X-ray diffraction. The theory remains valid for large diffraction efficiencies where the incident wave is strongly depleted. It is applied to transmission holograms and to reflection holograms. Spatial modulations of both the refractive index and the absorption constant are allowed for. The effects of loss in the grating and of slanted fringes are also considered. Algebraic formulas and their numerical evaluations are given for the diffraction efficiencies and the angular and wavelength sensitivities of the various hologram types.

I. INTRODUCTION

Holographic recording in thick media ("volume recording") is of particular interest for high-capacity information storage,[1-3] for color holography[4] and for efficient white-light display of holograms.[5-9] The high efficiency of light conversion which is attainable with thick dielectric holograms is also important for microimaging, and it may make it practical to use holographic optical components (for example, gratings or fly's eye lenses) in a variety of optical systems.

In thick holograms it is light diffraction at or near the Bragg angle

which leads to efficient wavefront reconstruction. This is true for both transmission and reflection holograms, and both types are considered in this paper. The (volume) record of the holographic interference pattern (fringe pattern) usually takes the form of a spatial modulation of the absorption constant or the refractive index of the medium, or both. Modulations of the absorption constant are produced in conventional photographic emulsions and in photochromics, while newer materials, like dichromated gelatin[10,11] lithium niobate,[12] or photopolymer materials[13] yield modulations of the refractive index.

This paper considers the properties of all these types of thick (or "deep") holograms. Of particular interest is their efficiency of converting light into the useful reconstructed wave (diffraction efficiency) and the angular dependence of this diffraction efficiency as the incident light deviates from the Bragg angle. We are also interested in the wavelength dependence and in the way the diffraction properties are changed in the presence of loss or a slant of the fringe pattern with respect to the surface of the recording medium.

Leith and his associates, and Gabor and Stroke have already considered some of the properties of thick holograms, in particular the angular and the wavelength dependence of the diffracted light.[14,15] Their theories are essentially linear or perturbational theories which use the Kirchhoff integral or the first Born approximation with the basic assumption that the incident light wave is not disturbed by the diffraction process. Their results are valid as long as this assumption is good. For high diffraction efficiencies (like 90 percent) the incident wave is strongly depleted and another approach is called for. One such approach is to use electronic computers to solve the relevant complicated electromagnetic problem accurately. Results of such computations are available for special cases. Klein, Tipnis, and Hiedemann have computed data for light diffraction by ultrasonic waves,[16,17] and Burckhardt has reported results for dielectric hologram gratings.[18,19] The method of Bathia and Noble[20] is another approach in which they employed integral equations to analyze acoustic diffraction of light.

Yet another approach is the use of a coupled wave theory, which is the subject of this paper. Such a theory can predict the maximum possible efficiencies of the various hologram types (results which one cannot hope to obtain from linear theories), and the angular and wavelength dependence at high diffraction efficiencies. Following Phariseau,[21] coupled wave theories have been successfully used in the treatment of light diffraction by acoustic waves[22] and by electrooptic gratings[23] where very similar diffraction processes are at work as in holography.

Closely related to the diffraction in thick holograms are also the diffraction of electrons in lattices and the diffraction of X-rays in crystals. The dynamical theory of X-ray diffraction[24] is also a theory of coupled waves and its application to holography has already been suggested.[25]

We have earlier reported some of the results and an outline of the coupled wave theory for hologram gratings.[26,27] Here we propose to give further results and a more detailed account of the basic assumptions and the analysis. We give analytic formulas for the various hologram types as well as numerical evaluations which include results on the angular sensitivities and the influence of loss and slant.

For simplicity the analysis is restricted to the holographic record of *sinusoidal* fringe patterns which we call hologram gratings. To some degree a more complicated hologram can be regarded as a multiplicity of such hologram gratings.

II. COUPLED WAVE ANALYSIS

2.1 *Derivation of the Coupled Wave Equations*

The coupled wave theory assumes monochromatic light incident on the hologram grating at or near the Bragg angle and polarized perpendicular to the plane of incidence.* Only two significant light waves are assumed to be present in the grating: the incoming "reference" wave R and the outgoing "signal" wave S. Only these two waves obey the Bragg condition at least approximately, the other diffraction orders violate the Bragg condition strongly and are neglected. They should be of little influence on the energy interchange between S and R. The last assumption limits the validity of the coupled wave theory to *thick* hologram gratings. Section 6 gives a more detailed discussion of this limitation.

Figure 1 shows the model of a hologram grating which is used for our analysis. The z-axis is chosen perpendicular to the surfaces of the medium, the x-axis in the plane of incidence and parallel to the medium boundaries and the y-axis perpendicular to the paper. The fringe planes are oriented perpendicular to the plane of incidence and slanted with respect to the medium boundaries at an angle ϕ. The fringes are shown dotted. The grating vector $\mathbf{K}$ is oriented perpendicular to the fringe planes and is of length $K = 2\pi/\Lambda$, where Λ is the period of the grating. The same average dielectric constant is assumed for the region inside and outside the grating boundaries. The angle of incidence measured *in* the medium is θ.

* A generalization to parallel polarization is given in the appendix.

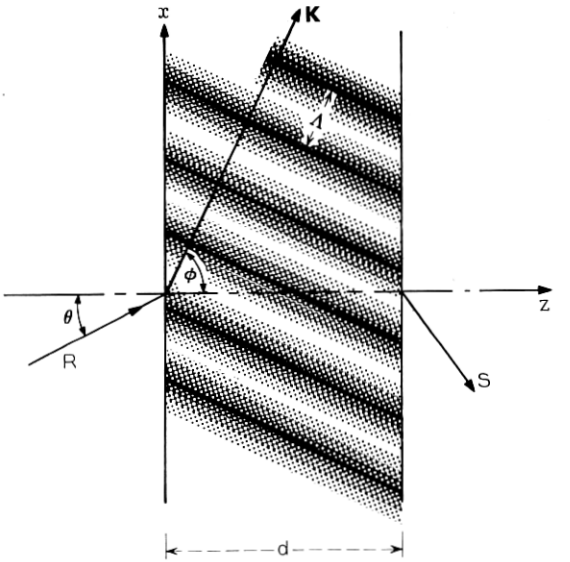

Fig. 1—Model of a thick hologram grating with slanted fringes. The spatial modulation of n or α is indicated by the dotted pattern. The grating parameters are: θ—angle of incidence in the medium, **K**—grating vector (perpendicular to the fringe planes), Λ—grating period, ϕ—slant angle, and d—grating thickness.

Wave propagation in the grating is described by the scalar wave equation

$$\nabla^2 E + k^2 E = 0, \tag{1}$$

where $E(x, z)$ is the complex amplitude of the y-component of the electric field, which is assumed to be independent of y and to oscillate with an angular frequency ω. The propagation constant $k(x, z)$ is spatially modulated and related to the *relative* dielectric constant $\epsilon(x, z)$ and the conductivity $\sigma(x, z)$ of the medium by

$$k^2 = \frac{\omega^2}{c^2}\epsilon - j\omega\mu\sigma \tag{2}$$

where c is the light velocity in free space and μ is the permeability of the medium which we assume to be equal to that of free space. In our model the constants of the medium are independent of y. The fringes of the hologram grating are represented by a spatial modulation of ϵ or σ:

$$\epsilon = \epsilon_0 + \epsilon_1 \cos(\mathbf{K}\cdot\mathbf{x})$$
$$\sigma = \sigma_0 + \sigma_1 \cos(\mathbf{K}\cdot\mathbf{x}) \tag{3}$$

where ϵ_1 and σ_1 are the amplitudes of the spatial modulation, ϵ_0 is the average dielectric constant and σ_0 the average conductivity. ϵ and σ are assumed to be modulated in phase. To simplify the notation we have used the radius vector $\mathbf{x}$ and the grating vector $\mathbf{K}$

$$\mathbf{x} = \begin{bmatrix} x \\ y \\ z \end{bmatrix}; \quad \mathbf{K} = K \begin{bmatrix} \sin\phi \\ 0 \\ \cos\phi \end{bmatrix}; \quad K = 2\pi/\Lambda.$$

Equations (2) and (3) can be combined in the form

$$k^2 = \beta^2 - 2j\alpha\beta + 2\kappa\beta(e^{i\mathbf{K}\cdot\mathbf{x}} + e^{-i\mathbf{K}\cdot\mathbf{x}}) \tag{4}$$

where we have introduced the average propagation constant β and the average absorption constant α:

$$\beta = 2\pi(\epsilon_0)^{\frac{1}{2}}/\lambda; \qquad \alpha = \mu c\sigma_0/2(\epsilon_0)^{\frac{1}{2}}, \tag{5}$$

and the coupling constant κ was defined as

$$\kappa = \frac{1}{4}\left(\frac{2\pi}{\lambda}\epsilon_1/(\epsilon_0)^{\frac{1}{2}} - j\mu c\sigma_1/(\epsilon_0)^{\frac{1}{2}}\right). \tag{6}$$

This coupling constant describes the coupling between the reference wave R and the signal wave S. It is the central parameter in the coupled wave theory. For $\kappa = 0$ there is no coupling between R and S and, therefore, there is no diffraction.

Optical media are usually characterized by their refractive index and their absorption constant. We also find it convenient to use these parameters if the following conditions are met

$$2\pi n/\lambda \gg \alpha; \qquad 2\pi n/\lambda \gg \alpha_1, \qquad n \gg n_1, \tag{7}$$

which is true in almost every practical case. Here n is the average refractive index, and n_1 and α_1 are the amplitudes of the spatial modulation of the refractive index and the absorption constant, respectively [compare equation (3)]. λ is the wavelength in free space. Under the above conditions we can write with good accuracy

$$\beta = 2\pi n/\lambda \tag{8}$$

and for the coupling constant

$$\kappa = \pi n_1/\lambda - j\alpha_1/2. \tag{9}$$

The spatial modulation indicated by n_1 or α_1 forms a grating which couples the two waves R and S and leads to an exchange of energy between them. We describe these waves by complex amplitudes $R(z)$ and $S(z)$ which vary along z as a result of this energy interchange or because of an energy loss from absorption. The total electric field in the grating is the superposition of the two waves:

$$E = R(z)e^{-i\mathfrak{p}\cdot\mathfrak{x}} + S(z)e^{-i\mathfrak{s}\cdot\mathfrak{x}}. \tag{10}$$

The propagation vectors $\mathfrak{p}$ and $\mathfrak{s}$ contain the information about the propagation constants and the directions of propagation of R and S. $\mathfrak{p}$ is assumed to be equal to the propagation vector of the free reference wave in the absence of coupling. $\mathfrak{s}$ is forced by the grating and related to $\mathfrak{p}$ and the grating vector by

$$\mathfrak{s} = \mathfrak{p} - \mathbf{K} \tag{11}$$

which has the appearance of a conservation of momentum equation. $\mathfrak{p}$ and $\mathfrak{s}$ have been chosen to conform as closely as possible with our picture of the physical process of the diffraction in the grating. If the actual phase velocities differ somewhat from the assumed values, then these differences will appear in the complex amplitudes $R(z)$ and $S(z)$ as a result of the theory.

Figure 2 shows the vectors of interest and their orientation. The components of $\mathfrak{p}$ are ρ_x and ρ_z which are given by

$$\mathfrak{p} = \begin{bmatrix} \rho_x \\ 0 \\ \rho_z \end{bmatrix} = \beta \begin{bmatrix} \sin\theta \\ 0 \\ \cos\theta \end{bmatrix}. \tag{12}$$

From this and equation (11) follow the $\mathfrak{s}$-components σ_x and σ_z

$$\mathfrak{s} = \begin{bmatrix} \sigma_x \\ 0 \\ \sigma_z \end{bmatrix} = \beta \begin{bmatrix} \sin\theta - \dfrac{K}{\beta}\sin\phi \\ 0 \\ \cos\theta - \dfrac{K}{\beta}\cos\phi \end{bmatrix}. \tag{13}$$

The vector relation (11) is shown in Fig. 3 together with a circle of radius β. The general case is shown in Fig. 3a, where the Bragg

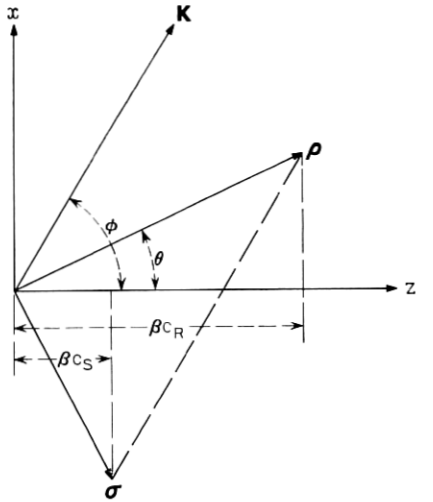

Fig. 2 — ϱ and σ, the propagation vectors of the reference wave R and the signal wave S, and their relation to the grating vector **K**. The obliquity factors c_R and c_S are indicated.

condition is not met and the length of σ differs from β. Figure 3b shows the same diagram for incidence at the Bragg angle θ_0 . In this special case the lengths of both, ϱ and σ are equal to the free propagation constant β, and the Bragg condition

$$\cos(\phi - \theta) = K/2\beta \tag{14}$$

is obeyed.

For a fixed wavelength the Bragg condition is violated by angular

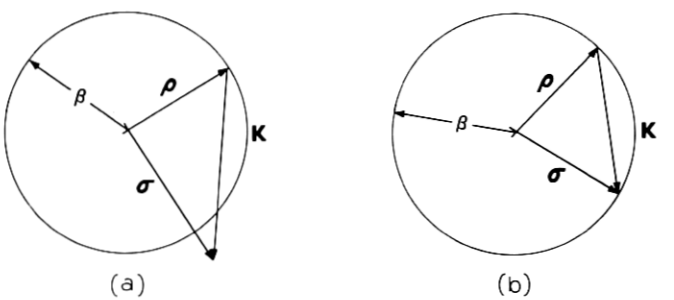

Fig. 3 — Vector diagram (conservation of momentum) for (a) near and (b) exact Bragg incidence.

deviations $\Delta\theta$ from the Bragg angle θ_0. For a fixed angle of incidence a similar violation takes place for changes $\Delta\lambda$ from the correct wavelength λ_0. We write

$$\theta = \theta_0 + \Delta\theta, \tag{15}$$

and

$$\lambda = \lambda_0 + \Delta\lambda,$$

and assume in the following that the deviations $\Delta\theta$ and $\Delta\lambda$ are small.

Angular changes $\Delta\theta$ have very similar effects on the behavior of the grating as wavelength changes $\Delta\lambda$, and there is a close relation between the angular sensitivity and the wavelength sensitivity of thick hologram gratings. We get an idea of this relationship by differentiating the Bragg condition (14), from which results

$$\frac{d\theta_0}{d\lambda_0} = K/4\pi n \sin(\phi - \theta_0). \tag{16}$$

The $\theta - \lambda$ connection shows up in the dephasing measure ϑ which appears in the coupled wave equations and which is defined by

$$\vartheta \equiv (\beta^2 - \sigma^2)/2\beta = K\cos(\phi - \theta) - \frac{K^2}{4\pi n}\lambda \tag{17}$$

and which has been expressed in this form using equation (13). A Taylor series expansion of equation (17) yields the following expression for ϑ which is correct to the first order in the deviations $\Delta\theta$ and $\Delta\lambda$:

$$\vartheta = \Delta\theta \cdot K \sin(\phi - \theta_0) - \Delta\lambda \cdot K^2/4\pi n. \tag{18}$$

Note that the deviations $\Delta\theta$ and $\Delta\lambda$ which produce equal dephasing ϑ are related by equation (16).

We are now ready to derive the coupled wave equations. We combine equations (1) and (4), and insert the expressions of (10) and (11). Then we compare the terms with equal exponentials ($e^{-i\varrho\cdot\mathbf{x}}$ and $e^{-i\mathfrak{d}\cdot\mathbf{x}}$) and arrive at

$$R'' - 2jR'\rho_z - 2j\alpha\beta R + 2\kappa\beta S = 0 \tag{19}$$

and

$$S'' - 2jS'\sigma_z - 2j\alpha\beta S + (\beta^2 - \sigma^2)S + 2\kappa\beta R = 0, \tag{20}$$

where the primes indicate differentiation with respect to z. The waves generated in the directions of $\varrho + \mathbf{K}$ and $\mathfrak{d} - \mathbf{K}$ are neglected, together with all other higher diffraction orders. In addition we assume that the

energy interchange between S and R is slow and that energy is absorbed slowly, if at all. This allows us to neglect R'' and S''. We will check the results of the theory later for a more detailed justification of this last step. We can now introduce equation (18) and rewrite the above equations in the form

$$c_R R' + \alpha R = -j\kappa S \tag{21}$$

$$c_S S' + (\alpha + j\vartheta) S = -j\kappa R. \tag{22}$$

These are the coupled wave equations which are the basis for our analysis. The abbreviations c_R and c_S stand for the expressions

$$\begin{aligned} c_R &= \rho_z/\beta = \cos\theta \\ c_S &= \sigma_z/\beta = \cos\theta - \frac{K}{\beta}\cos\phi. \end{aligned} \tag{23}$$

Our physical picture of the diffraction process is reflected in the coupled wave equations. A wave changes in amplitude along z because of coupling to the other wave (κR, κS) or absorption (αR, αS). For deviations from the Bragg condition S is forced out of synchronism with R and the interaction decreases (ϑS).

The energy balance of the coupled-wave model is described by the relation

$$(c_R RR^* + c_S SS^*)' + 2\alpha(RR^* + SS^*) + j(\kappa - \kappa^*)(RS^* + R^*S) = 0 \tag{24}$$

where the asterisk denotes a complex conjugate. This is easily derived from equations (21) and (22) by multiplying them with R^* and S^*, respectively, and adding the results together with the complex conjugate results. The presence of the obliquity factors c_R and c_S in the first part of equation (24) indicates that it is the power flow of the two waves *in the z direction* that enters the energy balance. In the absence of ohmic loss this power flow is conserved. The second and the third part in the equation describe the energy loss resulting from absorption in the grating. They correspond to the relevant terms of σEE^*.

2.2 *Solution of the Coupled Wave Equations*

It is straight forward to obtain the general solution of the coupled wave equations, which is

$$R(z) = r_1 \exp(\gamma_1 z) + r_2 \exp(\gamma_2 z) \tag{25}$$

$$S(z) = s_1 \exp(\gamma_1 z) + s_2 \exp(\gamma_2 z) \tag{26}$$

where the r_i and s_i are constants which depend on the boundary conditions. To determine the constants γ_i we insert equations (25) and (26) into the coupled wave equations and obtain

$$(c_R\gamma_i + \alpha)r_i = -j\kappa s_i \qquad (27)$$

$$i = 1, 2$$

$$(c_S\gamma_i + \alpha + j\vartheta)s_i = -j\kappa r_i \,. \qquad (28)$$

After multiplying the equations with each other we get a quadratic equation for γ_i

$$(c_R\gamma_i + \alpha)(c_S\gamma_i + \alpha + j\vartheta) = -\kappa^2, \qquad (29)$$

with the solution

$$\gamma_{1,2} = -\frac{1}{2}\left(\frac{\alpha}{c_R} + \frac{\alpha}{c_S} + j\frac{\vartheta}{c_S}\right) \pm \frac{1}{2}\left[\left(\frac{\alpha}{c_R} - \frac{\alpha}{c_S} - j\frac{\vartheta}{c_S}\right)^2 - 4\frac{\kappa^2}{c_R c_S}\right]^{\frac{1}{2}}. \qquad (30)$$

At this point we divert briefly from the main derivation, because now we have the means to check the validity of neglecting R'' and S'' in Section 2.1. This step is justified if the conditions $R'' \ll \zeta_z R'$, and $S'' \ll \sigma_z S'$ are obeyed. In view of equations (25) and (26) this will happen if $\gamma_i \ll \beta$. According to equation (30) the above requirement is met if $\Delta\theta \ll 1$ and if the inequalities of equation (7) are satisfied (which is usually the case).

Continuing the coupled wave analysis, we have to determine the constants r_i and s_i . To do this we have to introduce boundary conditions into our model. These are different for transmission holograms and for reflection holograms. Figure 4 gives an indication of this. For both hologram types the reference wave R is assumed to start with unit amplitude at $z = 0$. It decays as it propagates to the right and couples energy into S. In transmission holograms the signal S starts out with zero amplitude at $z = 0$ and propagates to the right ($c_S > 0$). In reflection holograms the signal travels to the left ($c_S < 0$) and it starts with zero amplitude at $z = d$.

Let us first analyze transmission holograms where $c_S > 0$. Here, the boundary conditions are

$$R(0) = 1, \qquad S(0) = 0 \qquad (31)$$

as discussed before. If we insert these boundary conditions into equa-

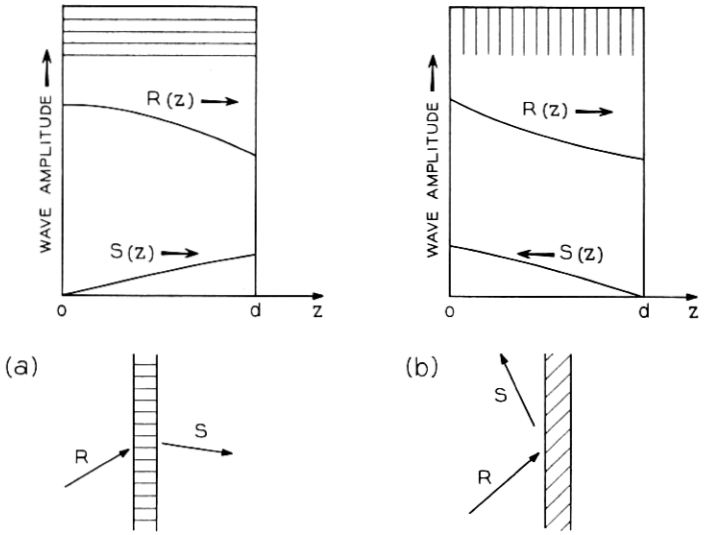

Fig. 4—Wave propagation in (a) transmission and (b) reflection holograms. The reference wave R decays while it propagates to the right. In (a) the signal S travels to the right and gains with z, while in (b) S travels to the left and gains with decreasing z. The shading indicates the orientation of the fringes.

tions (25) and (26),it follows immediately that

$$r_1 + r_2 = 1,$$

and (32)

$$s_1 + s_2 = 0.$$

Combining these relations with equation (28) we obtain

$$s_1 = -s_2 = -j\kappa/c_S(\gamma_1 - \gamma_2). \tag{33}$$

Introducing these constants in equation (26) we arrive at an expression for the amplitude of the signal wave at the output of the grating

$$S(d) = j\frac{\kappa}{c_S(\gamma_1 - \gamma_2)}(\exp(\gamma_2 d) - \exp(\gamma_1 d)). \tag{34}$$

This is a general expression, which is valid for all types of thick transmission holograms including the cases of off-Bragg incidence, of lossy gratings and of slanted fringe planes.

The analysis of reflection holograms follows a pattern similar to the above. We have $c_S < 0$ and boundary conditions given by

$$R(0) = 1, \qquad S(d) = 0. \tag{35}$$

The output plane for the signal wave is, now, at $z = 0$, and $S(0)$ is the output amplitude of interest. Inserting the boundary conditions in equations (25) and (26) yields

$$r_1 + r_2 = 1$$

and

$$s_1 \exp(\gamma_1 d) + s_2 \exp(\gamma_2 d) = 0. \tag{36}$$

To proceed with our derivation we rewrite the above relation for s_1 and s_2 in the form

$$\begin{aligned} s_1(\exp(\gamma_2 d) - \exp(\gamma_1 d)) &= (s_1 + s_2)\exp(\gamma_2 d) \\ s_2(\exp(\gamma_2 d) - \exp(\gamma_1 d)) &= -(s_1 + s_2)\exp(\gamma_1 d). \end{aligned} \tag{37}$$

Then we sum equation (28) for $i = 1$ and $i = 2$ and obtain the relation

$$-j\kappa(r_1 + r_2) = -j\kappa = (s_1 + s_2)(\alpha + j\vartheta) + c_S(\gamma_1 s_1 + \gamma_2 s_2). \tag{38}$$

Using the relations (37) to substitute the sum $(s_1 + s_2)$ for the terms s_1 and s_2 in this equation we finally arrive at the result for the amplitude $S(0)$ of the output signal of a reflection hologram

$$S(0) = s_1 + s_2 = -j\kappa \Big/ \left\{\alpha + j\vartheta + c_S \frac{\gamma_1 \exp(\gamma_2 d) - \gamma_2 \exp(\gamma_1 d)}{\exp(\gamma_2 d) - \exp(\gamma_1 d)}\right\}. \tag{39}$$

This is, again, a formula of quite general validity, including off-Bragg incidence, loss, and slant.

In the following sections we discuss the behavior of transmission and reflection holograms in greater detail, using the general formulas derived above. In these discussions a parameter of prime interest is the diffraction efficiency η, which is defined as

$$\eta = \frac{|c_S|}{c_R} SS^* \tag{40}$$

where S is the (complex) amplitude of the output signal for a reference wave R incident with unit amplitude. η is the fraction of the incident light power which is diffracted into the signal wave. S is equal to $S(d)$ for transmission holograms and equal to $S(0)$ for reflection holograms in the notation of this section. But for reasons of simplicity we omit the arguments in the following sections. The obliquity factors c_R and c_S appear in the above definition for the same reason they have appeared in the energy balance of equation (24): in the absence of loss it is the power flow in the z direction which is conserved.

For slanted gratings another important parameter is the slant factor c which is defined as the ratio between the obliquity factors

$$c = c_R/c_S = -\cos\theta/\cos(\theta_0 - 2\phi)$$

which we have expressed here, for Bragg incidence, in terms of the angle of incidence θ_0 and the slant angle ϕ. Figure 5 indicates lines of constant c as a function of θ_0 and ϕ. For transmission holograms c is positive ($c > 0$), and for reflection holograms c is negative ($c < 0$). In the diagram transmission and reflection holograms are separated by the line for $c = \infty$.

III. TRANSMISSION HOLOGRAMS

In this section we discuss transmission holograms in greater detail. We give algebraic formulas and their numerical evaluations for the diffraction efficiencies and the angular and wavelength sensitivities of dielectric and of absorption gratings. This includes results on the influence of loss and slant.

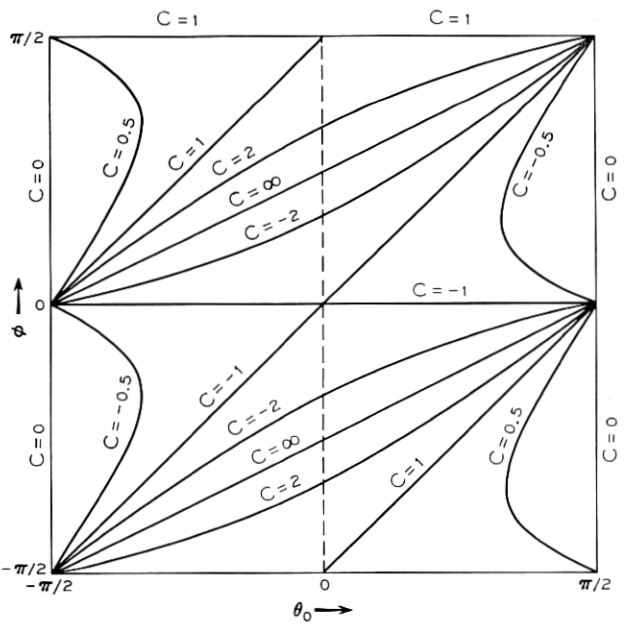

Fig. 5 — The slant factor c as a function of the angle of incidence θ_0 and the slant angle ϕ. c is positive for transmission holograms and negative for reflection holograms.

It is convenient to write the various diffraction formulas in terms of parameters ν and ξ, which are redefined for each grating type. In these parameters are lumped together the constants of the medium (n, α, n_1 , α_1 , κ), the obliquity factors (c_R , c_S), the wavelength, the grating thickness d, and the dephasing measure ϑ. By using ν and ξ, various trade-offs become immediately apparent.

We recall that, for transmission holograms, c_S is positive and the output signal appears at $z = d$. Combining equations (30) and (34) we obtain a general formula for the signal amplitude S of a transmission grating

$$\begin{aligned} S &= -j\left(\frac{c_R}{c_S}\right)^{\frac{1}{2}} \cdot \exp\,(-\alpha d/c_R) \cdot e^{\xi} \cdot \sin\,[\nu^2 - \xi^2]^{\frac{1}{2}}/[1 - \xi^2/\nu^2]^{\frac{1}{2}}, \\ \nu &= \kappa d/(c_R c_S)^{\frac{1}{2}}, \\ \xi &= \tfrac{1}{2} d\left(\frac{\alpha}{c_R} - \frac{\alpha}{c_S} - j\frac{\vartheta}{c_S}\right), \end{aligned} \tag{41}$$

where κ is the coupling constant given in equation (9), ϑ the dephasing measure of equation (18), c_R and c_S are the obliquity factors of equation (23), α is the absorption constant and d the grating thickness. In the above form the parameters ν and ξ are, in general, of complex value.

3.1 *Lossless Dielectric Gratings*

For completeness we give the formulas for the lossless dielectric grating. For the unslanted case of this grating these formulas have been previously obtained by several workers whose prime interest was light diffraction by acoustic waves.[20,21,28] For this grating type it is easy to include the effect of slanted fringes.* For the lossless dielectric grating we have a coupling constant $\kappa = \pi n_1/\lambda$ and $\alpha = \alpha_1 = 0$. Equation (41) can be rewritten in the form

$$\begin{aligned} S &= -j\left(\frac{c_R}{c_S}\right)^{\frac{1}{2}} e^{-j\xi} \sin\,(\nu^2 + \xi^2)^{\frac{1}{2}}/(1 + \xi^2/\nu^2)^{\frac{1}{2}}, \\ \nu &= \pi n_1 d/\lambda (c_R c_S)^{\frac{1}{2}}, \\ \xi &= \vartheta d/2c_S \end{aligned} \tag{42}$$

where ν and ξ have been redefined and are real-valued. The associated formula for the diffraction efficiency is

* Slant was also included in the treatment of dielectric gratings in Ref. 29.

$$\eta = \sin^2 (\nu^2 + \xi^2)^{\frac{1}{2}}/(1 + \xi^2/\nu^2). \tag{43}$$

For significant deviations from the Bragg condition the parameters ν and ξ are of equal order of magnitude, and we can take ν as independent of $\Delta\theta$ or $\Delta\lambda$ without causing an appreciable change in the predictions of equation (43). In this equation the angular and wavelength deviations are represented by the parameter ξ which can be written in the form

$$\begin{aligned} \xi &= \Delta\theta \cdot Kd \sin (\phi - \theta_0)/2c_s \\ &= -\Delta\lambda \cdot K^2 d/8\pi n c_s \end{aligned} \tag{44}$$

by using equation (18).

The angular and wavelength sensitivities of lossless dielectric gratings are shown in Fig. 6, where the efficiencies as given by equation (43) are plotted (normalized) as a function of ξ for three values of ν. The figure shows the sensitivity of gratings with $\nu = \pi/4$ and a peak diffraction efficiency of $\eta_0 = 0.5$, with $\nu = \pi/2$ and a peak efficiency of $\eta_0 = 1$, and with $\nu = 3\pi/4$ and $\eta_0 = 0.5$. We notice that the half-power points are reached for values near $\xi = 1.5$. There is some narrowing in the sensitivity curves for increasing values of ν, and a marked increase in the side lobe intensity.

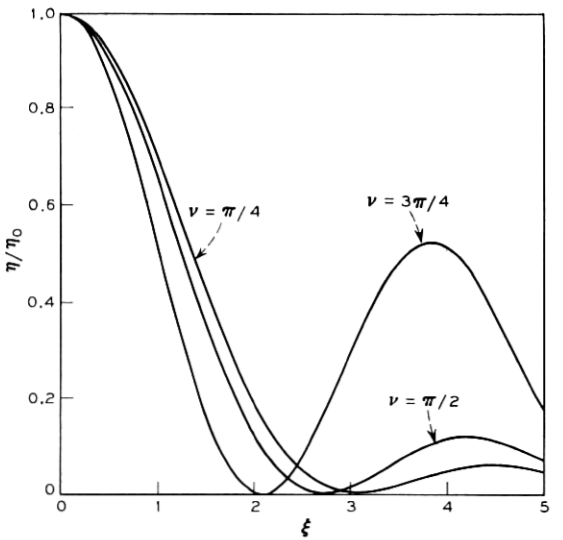

Fig. 6—Transmission holograms—the angular and wavelength sensitivity of lossless dielectric gratings with the normalized efficiencies η/η_0 as a function of ξ.

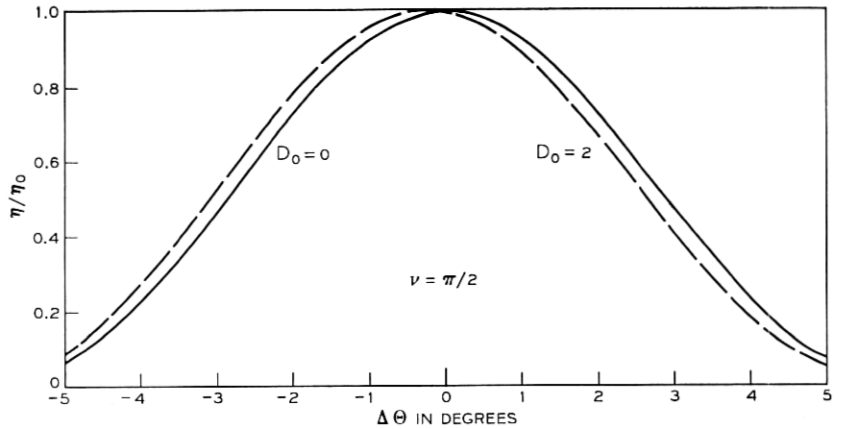

Fig. 7—Transmission holograms—the angular sensitivity of a lossy dielectric grating with $\nu = \pi/2$ and $D_0 = 2$ compared with that of a lossless dielectric grating ($D_0 = 0$), for $\theta_0 = 30°$ and $\beta d = 50$.

The above formulas include the influence of slant through the obliquity factors c_R and c_S. If there is no slant ($\phi = \pi/2$) and if the Bragg condition is obeyed then $c_R = c_S = \cos \theta_0$ and equation (43) becomes the well known[20,21,30]

$$\eta = \sin^2 (\pi n_1 d/\lambda \cos \theta_0). \tag{45}$$

By inserting the above half-power values for ξ into equation (44) we obtain simple rules of thumb for the angular and spectral half-power bandwidths of unslanted gratings: $2\Delta\theta_{\frac{1}{2}} \approx \Lambda/d$, $2\Delta\lambda_{\frac{1}{2}}/\lambda \approx \cot \theta \cdot \Lambda/d$.

3.2 *Lossy Dielectric Gratings*

Let us first study the influence of loss on the angular sensitivity of a dielectric grating. We assume that there is no slant ($\phi = \pi/2$) and therefore $c_R = c_S = \cos \theta$. With this and a coupling constant of $\kappa = \pi n_1/\lambda$ we obtain from equation (41) for the signal amplitude

$$\begin{aligned} S &= -j \exp(-\alpha d/\cos \theta) \cdot e^{-i\xi} \cdot \sin (\nu^2 + \xi^2)^{\frac{1}{2}}/(1 + \xi^2/\nu^2)^{\frac{1}{2}} \\ \nu &= \pi n_1 d/\lambda \cos \theta \\ \xi &= \vartheta d/2 \cos \theta = \Delta\theta \cdot \beta d \sin \theta_0 \end{aligned} \tag{46}$$

where ν and ξ have been redefined, and ξ has been expressed in the needed form with the use of equations (14) and (18).

Equation (46) has a form similar to that of equation (42) except

for an additional exponential term containing the absorption constant α. This term decreases the peak efficiency and it changes the angular sensitivity of the grating. But this change is very small, even for high loss values, as illustrated in Fig. 7. This figure compares the angular sensitivitities of a lossless grating ($D_0 = 0$) with that of a grating of high loss ($D_0 = 2$) for a parameter value of $\nu = \pi/2$, a Bragg angle of $\theta_0 = 30°$, and an optical grating thickness of $\beta d = 2\pi n d/\lambda = 50$. The loss parameter D_0 was defined as

$$D_0 = \alpha d/\cos \theta_0 \tag{47}$$

which is closely related to the conventional photographic density D (except that D_0 is measured in the direction of the reference wave given by θ_0). A value of $D_0 = 2$, which is the parameter used for the dashed curve, represents very high loss, with a decrease of the peak efficiency by a factor of about 50. Still, the differences of the two sensitivity curves are very small and consist mostly of an angular shift. The differences are even smaller for larger values of βd (we checked up to $\beta d = 200$), and, of course, for smaller values of D_0 . The main conclusion is that the presence of loss has very little influence on the angular sensitivity of a dielectric transmission grating. This is probably because absorption influences the phase relations between the waves R and S very little. It agrees with observations by Belvaux.[31]

Next let us consider the influence of loss on the efficiency of a slanted dielectric grating. For simplicity we assume Bragg incidence, that is, $\vartheta = 0$. The obliquity factors are positive and given by $c_R = \cos \theta_0$ and $c_S = -\cos(\theta_0 - 2\phi)$. For this case we can write equation (41) for the signal amplitude S in the form

$$\begin{aligned} S &= -j\left(\frac{c_R}{c_S}\right)^{\frac{1}{2}} \cdot \exp\left[-\tfrac{1}{2}D_0(1 + c)\right] \sin\left(\nu^2 - \xi^2\right)^{\frac{1}{2}}/\left(1 - \xi^2/\nu^2\right)^{\frac{1}{2}} \\ \nu &= \pi n_1 d/\lambda(c_R c_S)^{\frac{1}{2}} \\ \xi &= \tfrac{1}{2}D_0(1 - c) \end{aligned} \tag{48}$$

where we have used the loss parameter D_0 as above in equation (47), and the slant factor c

$$\begin{aligned} D_0 &= \alpha d/c_R = \alpha d/\cos \theta_0 \\ c &= c_R/c_S = -\cos \theta_0/\cos(\theta_0 - 2\phi). \end{aligned}$$

Figure 8 shows the diffraction efficiency of slanted grantings as calculated from equation (48). The efficiencies are plotted as a function

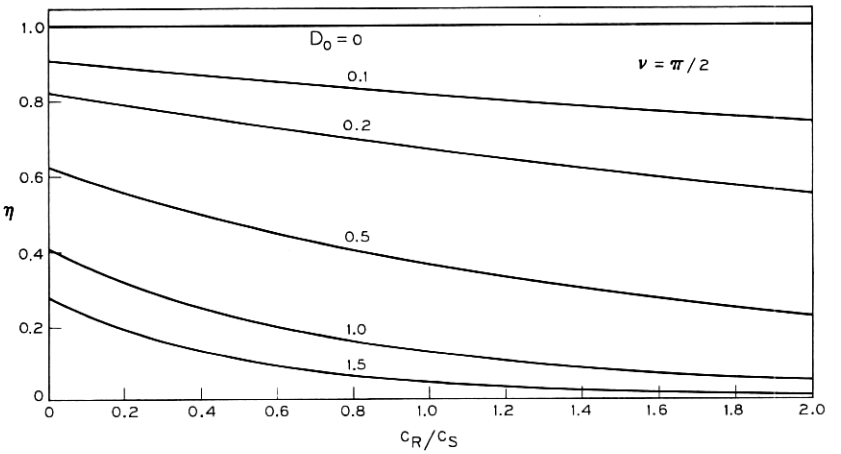

Fig. 8 — Transmission holograms—the efficiency of lossy dielectric gratings as a function of slant for $\nu = \pi/2$. $c = c_R/c_S$ is the slant factor.

of the slant factor c for various values of D_0 , and for a value of $\nu = \pi/2$ which corresponds to the maximum attainable efficiencies. Similar curves for $\nu = \pi/4$ and $\nu = 3\pi/4$ and the same D_0 values are almost identical to the curves of Fig. 8, except that the efficiency scale is reduced to a maximum efficiency of 0.5. This implies that for the range of chosen parameter values the exponential factor in equation (48) dominates in predicting the slant-dependence of the diffraction efficiency.

The results show that, for higher efficiencies, the grating prefers small c-values, assuming constant θ_0 and D_0 . This is a preference of small exist angles for S which means that we get the best efficiency if the signal wave leaves the grating on the shortest possible path after it has been generated.

3.3 *Unslanted Absorption Gratings*

When one records holograms in conventional photographic emulsions one produces absorption gratings (bleaching can convert this into a dielectric grating). In an absorption grating there is no spatial modulation of the refractive index ($n_1 = 0$) and the coupling is provided by a modulation (α_1) of the absorption constant. We have, then, an imaginary coupling constant $\kappa = -j\alpha_1/2$. In this section we study the efficiencies and the angular and wavelength sensitivities of unslanted absorption gratings where $\phi = \pi/2$ and $c_R = c_S = \cos\theta$. From equation (41) we obtain for the signal amplitude

$$S = -\exp(-\alpha d/c_R)\cdot e^{-i\xi}\cdot \mathrm{sh}\,(\nu^2 - \xi^2)^{\frac{1}{2}}/(1 - \xi^2/\nu^2)^{\frac{1}{2}}$$

$$\nu = \alpha_1 d/2\cos\theta \tag{49}$$

$$\xi = \vartheta d/2\cos\theta \approx \Delta\theta\cdot\beta d\cdot\sin\theta_0 = -\tfrac{1}{2}(\Delta\lambda/\lambda)Kd\tan\theta_0$$

where ν and ξ are real-valued, and equation (18) was used to express the parameter ξ again in various forms, showing explicitly the angular deviations $\Delta\theta$ and the wavelength deviation $\Delta\lambda$ from the Bragg condition.

For Bragg incidence we have $\xi = 0$, and obtain from the above a formula for the diffraction efficiency η of absorption gratings

$$\eta = \exp(-2\alpha d/\cos\theta_0)\cdot \mathrm{sh}^2\,(\alpha_1 d/2\cos\theta_0). \tag{50}$$

As we exclude the presence of negative absorption (gain) in the medium, there is an upper limit for the amplitude α_1 of the assumed sinusoidal modulation, which is $\alpha_1 \leqq \alpha$. The highest diffraction efficiency possible for an absorption grating is reached in the limiting case $\alpha_1 = \alpha$ for a value of $\alpha d/\cos\theta_0 = \ln 3$. According to equation (50) this maximum efficiency has a value of $\eta_{\max} = 1/27$, or 3.7 percent.

Figure 9 shows values for the diffracted amplitude S of absorption gratings as computed from equation (50) as a function of the modulation amplitude α_1 and for various values of the depth of modulation. For convenience we have again used loss parameters, which are $D_0 = \alpha d/\cos\theta_0$ and $D_1 = \alpha_1 d/\cos\theta_0$. D_1 is a measure for the amplitude of the spatial modulation and $D_0/D_1 = \alpha/\alpha_1$ indicates the modulation depth. The dashed curves for constant D_0 show the grating behavior for constant background absorption. We have plotted S on a linear scale in order to identify the regions of linear grating response. Note that a good linear response and relatively good efficiency is obtained if the absorption background is held constant to a value of about $D_0 = 1$.

Equation (49) predicts also the angular sensitivity and the frequency sensitivity of absorption gratings. Such sensitivity curves are plotted in Fig. 10 for the special case of $\alpha_1 = \alpha_0$ and values of $\nu \equiv D_1/2 = 1$ (dashed) and $\nu = \frac{1}{2}\ln 3 = 0.55$. For the latter parameter value the peak efficiency of 3.7 percent is reached, and for $\nu = 1$ we have a peak efficiency of 2.5 percent. In the figure the relative efficiencies are plotted as functions of the parameter ξ. We note that there is very little difference between the sensitivity curves for the two ν-values chosen. We have also computed the sensitivity for smaller values of ν (0.2, 0.4), but the resulting curves differ so little from the ones shown that we have omitted them from the figure. The sensitivity curves are very

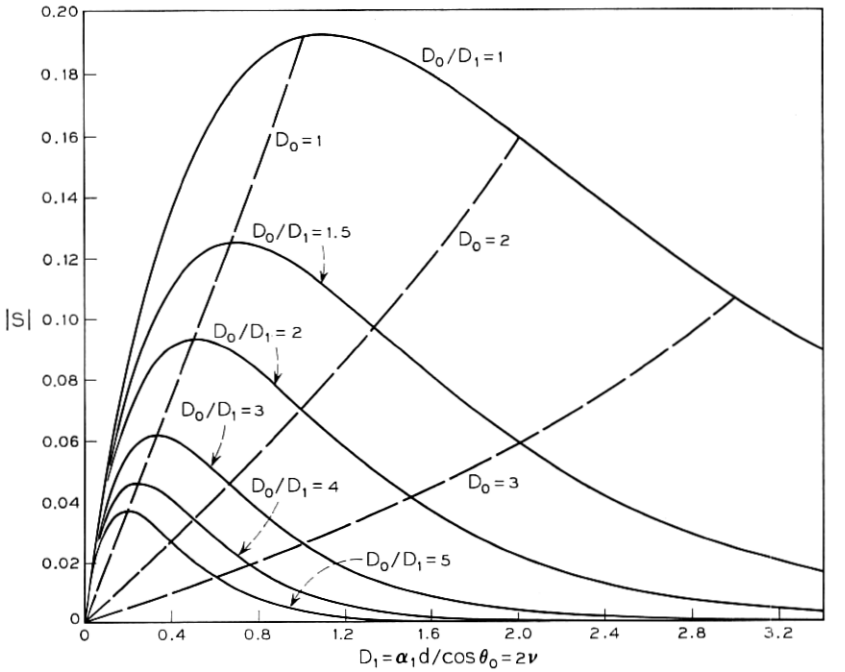

Fig. 9. — Transmission holograms—the diffracted amplitude of an absorption grating as a function of the modulation $D_1 = \alpha_1 d/\cos\theta = 2\nu$ for various modulation depths D_1/D_0 (solid curve) and various bias levels $D_0 = \alpha d/\cos\theta$ (dashed curve).

similar to those of the dielectric gratings with smaller ν-values which are shown in Fig. 6. Again, the half-power points are reached for about $\xi = 1.5$. But for absorption gratings there is no narrowing with increasing values of ν, and the side lobe intensity remains low.

3.4 *Slanted Absorption Gratings*

In this section we consider the influence of slant on the efficiency of an absorption grating. For simplicity we assume Bragg incidence ($\vartheta = 0$), and describe the slant by the obliquity factors $c_R = \cos\theta_0$ and $c_S = \cos(\theta_0 - 2\phi)$, as before. Using equation (41) we obtain, for this case, the following expression for the signal amplitude S

$$S = -\left(\frac{c_R}{c_S}\right)^{\frac{1}{2}} \exp\left[-\frac{1}{2}\alpha d\left(\frac{1}{c_R} + \frac{1}{c_S}\right)\right] \operatorname{sh}(\nu^2 + \xi^2)^{\frac{1}{2}}/(1 + \xi^2/\nu^2)^{\frac{1}{2}}$$

$$\nu = \alpha_1 d/2(c_R c_S)^{\frac{1}{2}} \tag{51}$$

$$\xi = \tfrac{1}{2}\alpha d\left(\frac{1}{c_R} - \frac{1}{c_S}\right),$$

where ν and ξ are redefined as real parameters. We have plotted the slant-dependence of absorption gratings in Fig. 11 for the special case of $\alpha_1 = \alpha$, that is, maximum depth of modulation. The diffraction efficiency η is shown as a function of the slant factor c for various values of the loss parameter D_0 . These quantities are defined, as before, by

$$D_0 = \alpha d/c_R = \alpha d/\cos\theta_0$$

and (52)

$$c = c_R/c_S .$$

The efficiency is seen to reach its absolute maximum of 3.7 percent for the unslanted grating ($c = 1$) and for a loss parameter of $D_0 = \ln 3$. For larger values of D_0 the efficiencies reach relative maxima for exit

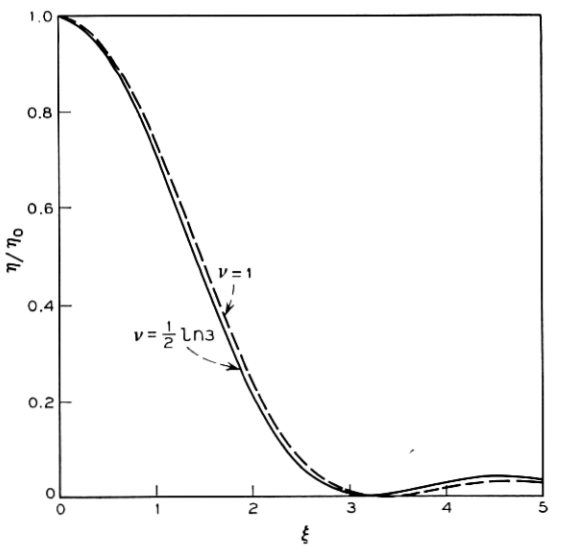

Fig. 10—Transmission holograms—the angular and wavelength sensitivity of an absorption grating for $\alpha_1 = \alpha$ ($D_1 = D_0$) and values of $\nu = D_1/2 = 0.55$ ($\eta_0 = 0.037$) and $\nu = D_1/2 = 1$ ($\eta_0 = 0.025$).

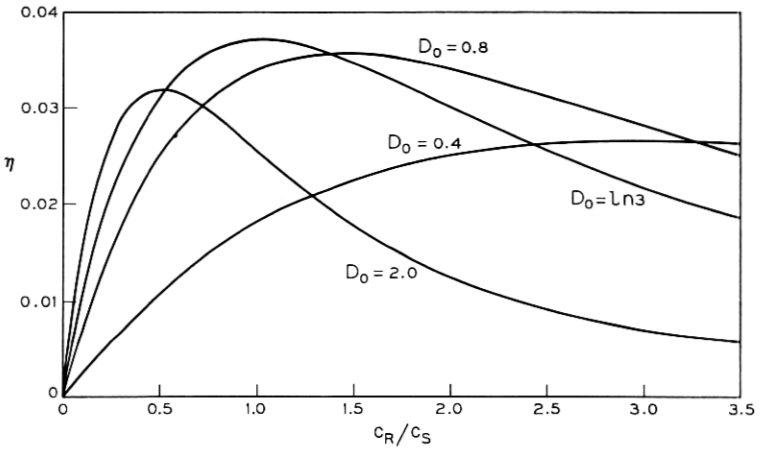

Fig. 11 — Transmission holograms—the efficiency of an absorption grating as a function of slant for $\alpha_1 = \alpha$ ($D_1 = D_0$). $c = c_R/c_S$ is the slant factor.

angles of the signal wave which are smaller than that of the reference wave ($c < 1$), while for smaller D_0-values the situation is reversed.

3.5 *Mixed Gratings*

Mixed gratings are those in which both the refractive index and the absorption constant are spatially modulated. This may occur in some recording materials (for example, as a result of incomplete bleaching, or in cases where strong absorption peaks are developed which cause refractive index changes according to the Kramers–Kronig relations).* Mixed gratings are described by a complex coupling constant, which is given in equation (9). For the special case of unslanted gratings ($\phi = \pi/2$) and Bragg incidence ($\vartheta = 0$) equation (41) simplifies to

$$S = -j \exp(-\alpha d/\cos\theta_0) \sin(\kappa d/\cos\theta_0) \tag{53}$$

where κ is complex. From this we obtain, after some algebra, an expression for the efficiency of mixed gratings

$$\eta = SS^* = [\sin^2(\pi n_1 d/\lambda \cos\theta_0) + \mathrm{sh}^2(\alpha_1/2 \cos\theta_0)] \exp(-2\alpha d/\cos\theta_0), \tag{54}$$

where n_1 and α_1 are the amplitudes of the modulation of the refractive index and the absorption constant, and α is the average absorption

* Such effects have recently been observed by Nassenstein (see Ref. 32).

constant. We note that, at least for the special case considered here, there is a simple addition of the intensities diffracted by the dielectric grating and the absorption grating respectively [compare equations (46) and (50)!]. The exponential factor including α insures that the formula does not predict efficiencies larger than 1.

IV. REFLECTION HOLOGRAMS

In reflection holograms the recorded fringe-planes are of an orientation which is more or less parallel to the surfaces of the recording medium, and the signal appears as a "reflection" of the reference wave. We have illustrated this situation in Fig. 4b. It is expressed in the coupled wave analysis by negative values of the obliquity factor $c_S (c_S < 0)$. In addition, the signal amplitude S of interest is obtained by evaluating the signal wave in the plane $z = 0$, which is also the entrance plane for the reference wave R. For reflection holograms a slant angle $\phi = 0$ describes the case of unslanted gratings. Apart from these differences the following discussion of the detailed behavior of reflection holograms proceeds in a pattern similar to that of Section III, where we have discussed transmission holograms.

From equations (30) and (39) we obtain a general formula for the signal amplitude of reflection holograms which can be written in the form

$$\begin{aligned} S &= \left(\frac{c_R}{c_S}\right)^{\frac{1}{2}} \cdot \operatorname{sh}(\nu \operatorname{ch} a)/\operatorname{ch}(a + \nu \operatorname{ch} a) \\ \nu &= j\kappa d/\lambda(c_R c_S)^{\frac{1}{2}} \\ \xi &= \tfrac{1}{2} d\left(\frac{\alpha}{c_R} - \frac{\alpha}{c_S} - j\frac{\vartheta}{c_S}\right) \\ \operatorname{sh} a &= \xi/\nu \end{aligned} \tag{55}$$

where we have again defined (complex) parameters ν, ξ and a, which lump together the constants of the medium $(n, \alpha, n_1, \alpha_1, \kappa)$, the obliquity factors c_R and c_S, the wavelength, the grating thickness d and the dephasing measure ϑ.

4.1 *Lossless Dielectric Gratings*

The lossless dielectric grating is characterized by a real-valued coupling constant $\kappa = \pi n_1/\lambda$, and by zero absorption $\alpha = \alpha_1 = 0$. As in the transmission-hologram counterpart, it is easy to include the case of slant in the analysis. For the present case we can rewrite equa-

tion (55) in the form

$$S = \left(\frac{c_R}{c_S}\right)^{\frac{1}{2}} / \{j\xi/\nu + (1 - \xi^2/\nu^2)^{\frac{1}{2}} \cdot \coth (\nu^2 - \xi^2)^{\frac{1}{2}}\}$$

$$\nu = j\pi n_1 d/\lambda(c_R c_S)^{\frac{1}{2}} \tag{56}$$

$$\xi = -\vartheta d/2c_S$$

where ν and ξ have been redefined as real-valued parameters (c_S is negative!).

The associated formula for the diffraction efficiency of lossless dielectric gratings is

$$\eta = 1/\{1 + (1 - \xi^2/\nu^2)/\mathrm{sh}^2 (\nu^2 - \xi^2)^{\frac{1}{2}}\}, \tag{57}$$

which also provides a description of the angular and wavelength sensensitivities of the grating. For unslanted acoustic gratings this formula has been previously given by Quate and his associates.[22] Sensitivity curves calculated from equation (57) are shown in Fig. 12, where the normalized efficiencies are plotted as a function of ξ for various values of ν = const. The figure shows the sensitivity of a grating with $\nu = \pi/4$ and a peak efficiency of 43 percent, a grating with $\nu = \pi/2$ and $\eta_0 = 0.84$,

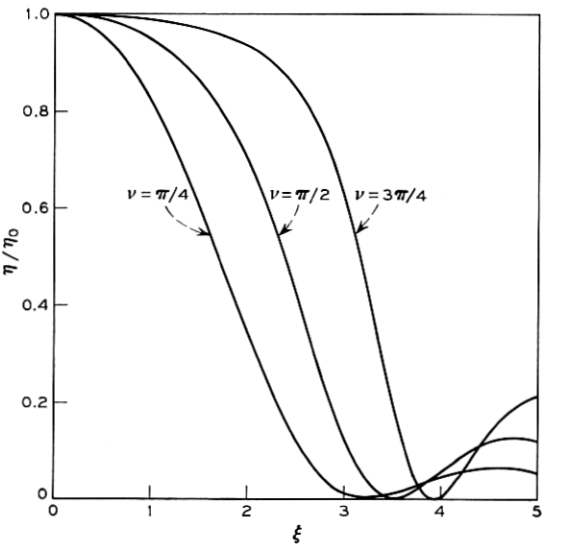

Fig. 12—Reflection holograms—the angular and wavelength sensitivity of a lossless dielectric grating with the normalized efficiency η/η_0 as a function of ξ.

and the corresponding values for $\nu = 3\pi/4$ and $\eta_0 = 0.96$. For $\nu = \pi/4$ the half-power points of the grating response are reached for values of approximately $\xi = 1.7$. But there is considerable broadening of the sensitivity curves for increasing values of ν, and an increase in the side-lobe level.

As in equation (44) for transmission holograms, we can express the parameter ξ directly in the angular deviation $\Delta\theta$ or the wavelength deviation $\Delta\lambda$ by using equation (18) to obtain

$$\begin{aligned} \xi &= \Delta\theta \cdot Kd \cdot \sin(\theta_0 - \phi)/2c_S \\ &= \Delta\lambda \cdot K^2 d/8\pi n c_S \ . \end{aligned} \tag{58}$$

These expressions can again be used to formulate rules for the angular bandwidth and the spectral bandwidth of the grating.

For an unslanted grating ($\phi = 0$) and Bragg incidence we have $c_R = -c_S = \cos\theta_0$, and equation (57) simplifies to

$$\eta = \text{th}^2(\pi n_1 d/\lambda \cos\theta_0). \tag{59}$$

This is a formula which has been obtained previously for light diffraction by acoustic waves.[33,22]

4.2 *Lossy Dielectric Gratings*

Let us first discuss the influence of loss on the angular and wavelength sensitivity of unslanted dielectric gratings. Here we have $\phi = 0$ and, to a good approximation

$$\begin{aligned} c_R &= \cos\theta_0(1 - \Delta\theta \tan\theta_0) = \cos\theta \\ c_S &= -\cos\theta_0(1 + \Delta\theta \tan\theta_0), \\ &= -\cos\theta(1 + 2\Delta\lambda/\lambda) \end{aligned} \tag{60}$$

at least as long $\tan\theta_0 \leqq 1$. One can show that the formula for the signal amplitude S, which we have given in equation (56), is still applicable for the present case of an unslanted lossy grating if we modify the parameters ν and ξ to

$$\begin{aligned} \nu &= \pi n_1 d/\lambda \cos\theta_0 \\ \xi &= \xi_0 - jD_0 \ , \\ \xi_0 &= -\Delta\theta \cdot \beta d \sin\theta_0 \\ D_0 &= \alpha d/\cos\theta_0 \end{aligned} \tag{61}$$

where ξ is now a complex parameter with ξ_0 describing the angular

deviations and D_0 representing the loss. An evaluation of this formula is shown in Fig. 13, which shows the angular sensitivity of dielectric gratings for various values of the loss parameter D_0 and a grating parameter of $\nu = \pi/2$. In constrast to what we have observed in the case of dielectric transmission holograms (Fig. 7), we see here a quite noticeable effect of the grating loss on the sensitivity curves. With increasing loss values the curves broaden in the wings, sharpen somewhat in the center and the side-lobe level decreases.

To study the influence of loss on the diffraction efficiencies of dielectric gratings we rewrite equation (55) in the form

$$\begin{aligned} S &= \left(\frac{c_R}{c_S}\right)^{\frac{1}{2}} / \{\xi/\nu + (1 + \xi^2/\nu^2)^{\frac{1}{2}} \cdot \coth (\nu^2 + \xi^2)^{\frac{1}{2}}\} \\ \nu &= j\pi n_1 d/\lambda(c_R c_S)^{\frac{1}{2}} \\ \xi &= \tfrac{1}{2} D_0(1 - c) \end{aligned} \tag{62}$$

where we have written ν and ξ as real-valued parameters in a form which is valid for Bragg incidence and for slanted or unslanted gratings. Just as in the case of transmission holograms we have used the loss

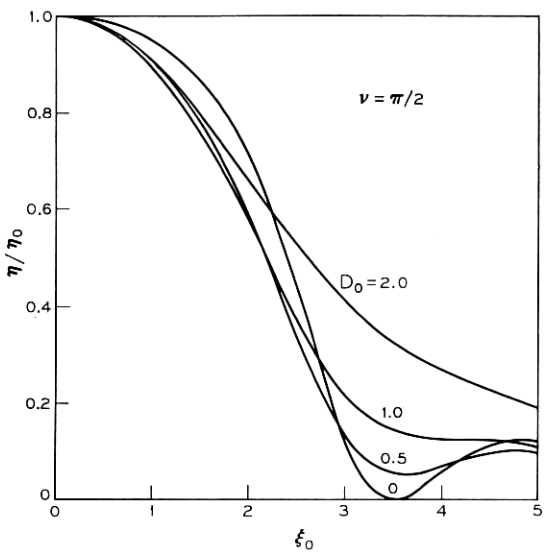

Fig. 13 — Reflection holograms—the influence of loss on the angular and wavelength sensitivity of a dielectric grating for $\nu = \pi/2$. The normalized efficiencies η/η_0 are shown. The peak efficiencies are $\eta_0 = 0.84$ for $D_0 = 0$, $\eta_0 = 0.64$ for $D_0 = 0.5$, $\eta_0 = 0.28$ for $D_0 = 1$, and $\eta_0 = 0.12$ for $D_0 = 2$.

parameter D_0 and the slant factor c (which is now negative)

$$D_0 = \alpha d/\cos\theta_0$$
$$c = c_R/c_S \ . \tag{63}$$

In the case of unslanted gratings the parameters ν and ξ simplify to

$$\nu = \pi n_1 d/\lambda \cos\theta_0$$
$$\xi = D_0 = \alpha d/\cos\theta_0 \ . \tag{64}$$

The results of a numerical evaluation for unslated gratings are shown in Fig. 14, where the signal amplitude is plotted as a function of ν for various values of the loss parameter D_0 . The curve $D_0 = 0$ gives the values for lossless gratings, while the others indicate the influence of loss.

The behavior of slanted dielectric gratings in the presence of loss is shown in Fig. 15. The curves of this figure are also computed from equation (62) and show the diffraction efficiency as a function of the slant factor for $\nu = \pi/2$ and various values of the loss parameter D_0 . For constant D_0 we notice an increase of the efficiency for decreasing values of the slant factor, as in the case of transmission holograms.

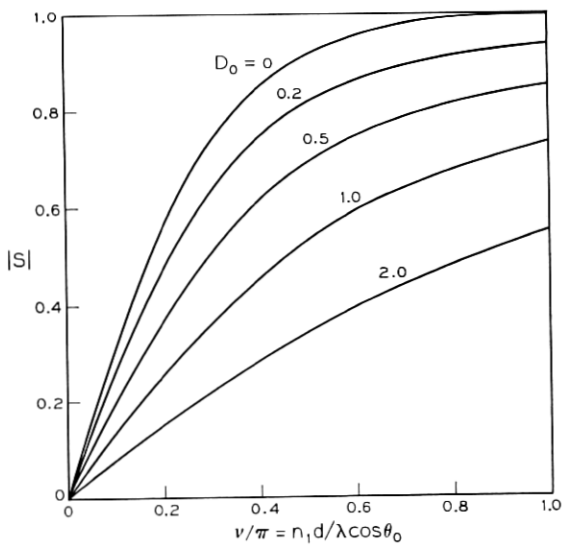

Fig. 14—Reflection holograms—the influence of loss on the diffracted amplitude S of an unslanted dielectric grating. $|S|$ is shown as a function of $\nu/\pi = n_1 d/\lambda \cos\theta_0$ for various loss parameters D_0.

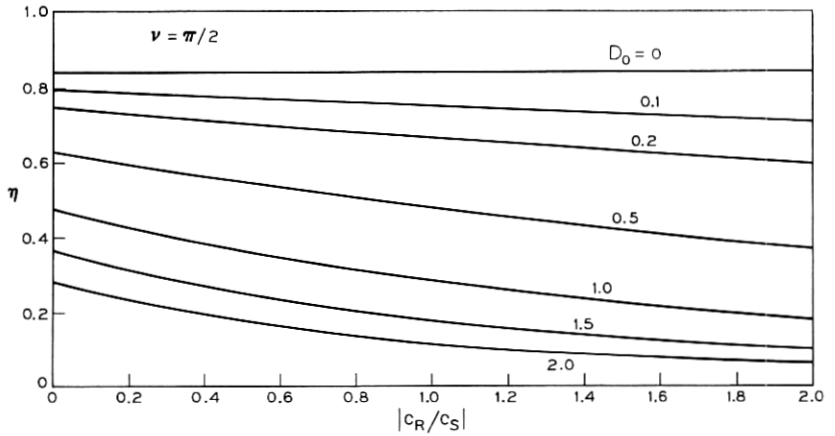

Fig. 15 — Reflection holograms—the efficiency of a lossy dielectric grating as a function of slant for $\nu = \pi/2$. $c = c_R/c_S$ is the slant factor.

Again, for given loss and a given angle of incidence short signal paths through the grating (that is, small exit angles) are preferred for higher efficiencies.

4.3 *Unslanted Absorption Gratings*

Following the pattern set in the discussion of transmission holograms (Section III), we again describe an absorption grating by an imaginary coupling constant $\kappa = -j\alpha_1/2$, and proceed to study the diffraction efficiencies and the angular and wavelength sensitivities of unslanted ($\phi = 0$) gratings. In this case equation (55) simplifies to

$$\begin{aligned} S &= -j\left(\frac{c_R}{c_S}\right)^{\frac{1}{2}} / \{\xi/\nu + [(\xi/\nu)^2 - 1]^{\frac{1}{2}} \coth (\xi^2 - \nu^2)^{\frac{1}{2}}\} \\ \nu &= j\alpha_1 d/2(c_R c_S)^{\frac{1}{2}} \\ \xi &= D_0 - j\xi_0 \end{aligned} \tag{65}$$

where the real-valued parameters D_0 and ξ_0 can be expressed to first order in the angular deviations $\Delta\theta$ and the wave-length deviations $\Delta\lambda$ by

$$\begin{aligned} D_0 &= \alpha d/\cos\theta_0 \\ \xi_0 &= \Delta\theta \cdot \beta d \sin\theta_0 = \tfrac{1}{2}(\Delta\lambda/\lambda)Kd. \end{aligned} \tag{66}$$

D_0 is a loss parameter as before, and ξ_0 is a normalized measure for the angular or the wavelength deviations from the Bragg condition.

If the Bragg condition is obeyed equation (65) can be written in the form

$$S = -D_1/2[D_0 + (D_0^2 - D_1^2/4)^{\frac{1}{2}} \cdot \coth (D_0^2 - D_1^2/4)^{\frac{1}{2}}] \qquad (67)$$

where

$$D_1 = 2\nu_1 = \alpha_1 d/\cos \theta_0$$

measures the spatial modulation of the absorption constant (α_1).

For the deepest allowable modulation where we have $D_1 = D_0(\alpha_1 = \alpha_0)$, this equation predicts the maximum diffraction efficiency η_{max} which is possible for reflection holograms with a (sinusoidal) absorption modulation. We obtain $\eta_{max} = 1/(2 + \sqrt{3})^2$, or a maximum efficiency of 7.2 percent for $D_0 = D_1 \to \infty$. The formula reflects the experimental fact that, for reflection holograms of the absorptive kind, one obtains the largest efficiencies for high photographic densities. Figure 16 shows a numerical evaluation of the above formula. Here the signal amplitude S is plotted as a function of the modulation amplitude D_1 for various levels of loss "bias" D_0 (dashed curves) and for various modulation depths D_0/D_1.

An evaluation of the grating sensitivity as predicted by equation (65) is shown in Fig. 17 for the special case of a maximum depth of modulation where $D_1 = D_0$. In this figure the (normalized) efficiency is plotted as a function of the parameter ξ_0 for various values of $D_1 = D_0$. As in the corresponding grating for the case of transmission holograms (Fig. 10) the sensitivity curves are seen to reach their half-power points for values of about $\xi_0 = 1.5$. But in the present case of reflection holograms there is a noticeable broadening of the curves with increasing loss values $D_1 = D_0$.

4.4 *Slanted Absorption Gratings*

In this section we consider the influence of slant on the diffraction efficiency of an absorption grating for reflection holograms. We assume Bragg incidence ($\vartheta = 0$) and again use the obliquity factors $c_R = \cos \theta_0$ and $c_S = -\cos (\theta_0 - 2\phi)$ to describe the slant (for reflection holograms we have $c_S < 0$!). We find that equation (65) can be used as a formula for the signal amplitude for the present case if we modify the parameters to

$$\nu = j\alpha_1 d/2(c_R c_S)^{\frac{1}{2}} = \frac{j}{2} D_1(c)^{\frac{1}{2}}$$

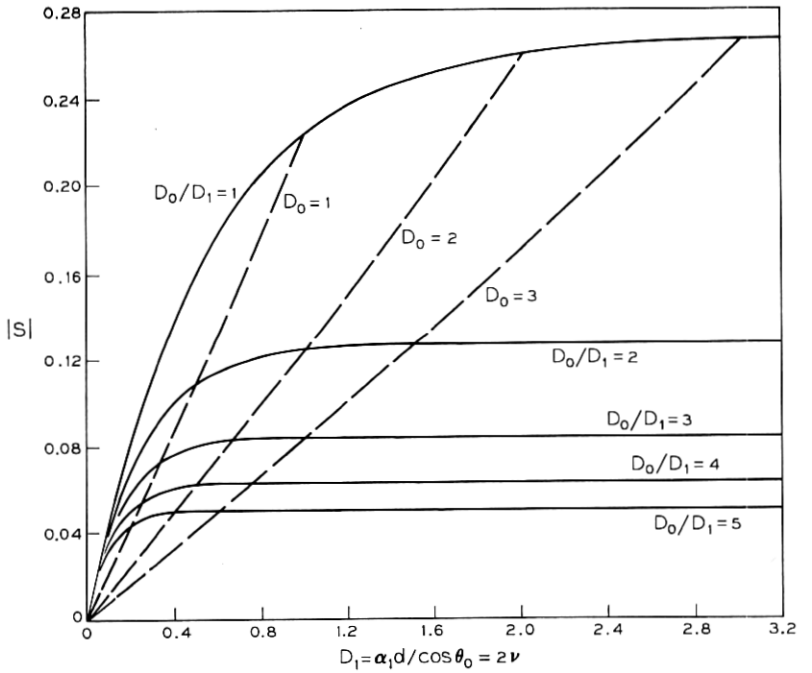

Fig. 16—Reflection holograms—the diffracted amplitude of an absorption grating as a function of the modulation $D_1 = \alpha_1 d/\cos\theta = 2\nu$ for modulation depths D_1/D_0 (solid curve) and bias levels $D_0 = \alpha d/\cos\theta$ (dashed curve).

$$\begin{aligned} \xi &= \tfrac{1}{2} D_0(1 - c) \\ D_0 &= \alpha d/\cos\theta_0 , \qquad D_1 = \alpha_1 d/\cos\theta_0 \\ c &= c_R/c_S \end{aligned} \tag{68}$$

where the slant factor c is negative. All these parameters are real-valued in the present case. For a maximum depth of modulation, that is, $\alpha_1 = \alpha$, there are further simplifications, and we obtain a simple expression for the slant-dependence of the diffraction efficiency

$$\eta = -c/\{1 - c + (1 - c + c^2)^{\frac{1}{2}} \cdot \coth \tfrac{1}{2} D_0(1 - c + c^2)^{\frac{1}{2}}\}^2. \tag{69}$$

Figure 18 shows a numerical evaluation of this formula for various values of $D_0 = D_1$. The slant factor value of $|\, c \,| = 1$ refers to unslanted gratings. In this case the maximum efficiency value $\eta_{\max} = 0.072$ is approached for large D_0. We note that for values of D_0 below unity

the efficiencies increase for $|\ c\ |$-values larger than 1 and up to about 3, that is, for relatively large exit angles of the signal wave.

4.5 *Mixed Gratings*

Mixed gratings are described by a complex coupling constant $\kappa = \pi n_1/\lambda - j\alpha_1/2$ (see Section 3.5). For Bragg incidence ($\vartheta = 0$) and unslanted fringe-planes ($\phi = 0$) we can obtain from equation (55) a formula for the signal amplitude of mixed gratings, which is

$$S = -j\kappa \Big/ \left\{ \alpha + (\kappa^2 + \alpha^2)^{\frac{1}{2}} \cdot \coth \frac{d}{\cos \theta_0} (\kappa^2 + \alpha^2)^{\frac{1}{2}} \right\} \tag{70}$$

where κ is of complex value, α is the average absorption constant, d the grating thickness and θ_0 the angle of incidence.

V. AMPLITUDES OF THE DIRECT WAVES

For diagnostic purposes it is often of interest to monitor the change in amplitude of the direct reference wave R, which is depleted because of diffraction into S and absorption. The quantities of interest are the amplitudes $R(d)$ which can be obtained from the analysis of Section 2.2.

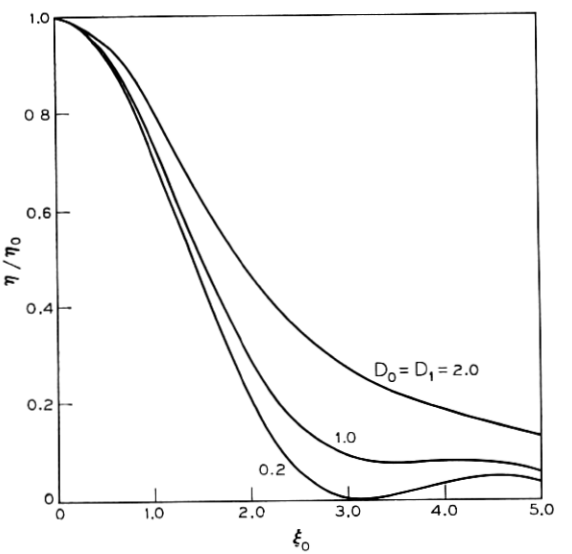

Fig. 17 — Reflection holograms—the angular and wavelength sensitivity of an absorption grating for $\alpha_1 = \alpha$ ($D_1 = D_0$) and values of $D_1 = 2\nu = D_0 = 0.2$ ($\eta_0 = 0.007$), $D_1 = 1$ ($\eta_0 = 0.05$), and $D_1 = 2$ ($\eta_0 = 0.068$).

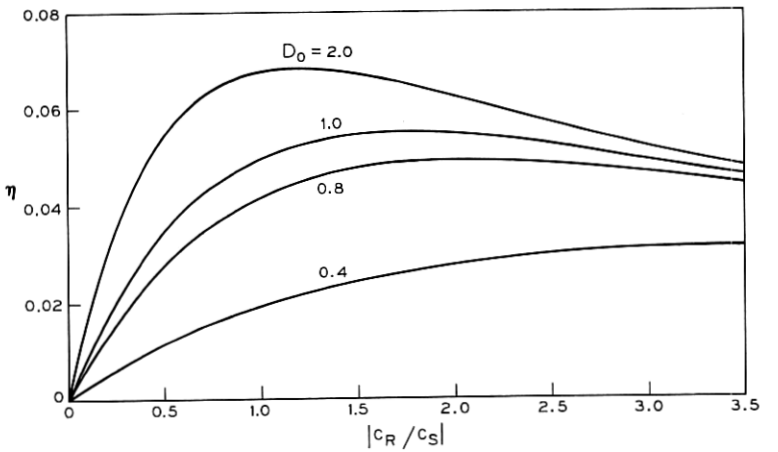

Fig. 18—Reflection holograms—the efficiency of an absorption grating as a function of slant for $\alpha_1 = \alpha$ ($D_1 = D_0$). $c = c_R/c_S$ is the slant factor.

We will give here the general results for transmission and reflection holograms. The notation is that of Section 2.

5.1 *Transmission Holograms*

From equations (27) and (33) we get for the constants r_i of equation (25) the expressions

$$\begin{aligned} r_1 &= -\kappa^2/c_S(\gamma_1 - \gamma_2)(c_R\gamma_1 + \alpha) \\ r_2 &= \kappa^2/c_S(\gamma_1 - \gamma_2)(c_R\gamma_2 + \alpha). \end{aligned} \tag{71}$$

Using this we can write the output amplitude $R(d)$ of the reference wave in the form

$$R(d) = \frac{\kappa^2}{c_S(\gamma_1 - \gamma_2)}\left(\frac{\exp(\gamma_2 d)}{c_R\gamma_2 + \alpha} - \frac{\exp(\gamma_1 d)}{c_R\gamma_1 + \alpha}\right). \tag{72}$$

5.2 *Reflection Holograms*

For reflection holograms we use equations (27), (37), and (39) to express the constants r_i in the form

$$\begin{aligned} r_1 &= (c_S\gamma_1 + \alpha + j\vartheta)\exp(\gamma_2 d)/\{\exp(\gamma_2 d)(\alpha + j\vartheta + c_S\gamma_1) \\ &\qquad - \exp(\gamma_1 d)(\alpha + j\vartheta + c_S\gamma_2)\} \\ r_2 &= -(c_S\gamma_2 + \alpha + j\vartheta)\exp(\gamma_1 d)/\{\exp(\gamma_2 d)(\alpha + j\vartheta + c_S\gamma_1) \\ &\qquad - \exp(\gamma_1 d)(\alpha + j\vartheta + c_S\gamma_2)\}. \end{aligned} \tag{73}$$

The output amplitude $R(d)$ of the reference wave becomes

$$R(d) = c_S(\gamma_1 - \gamma_2)/\{(\alpha + j\vartheta + c_S\gamma_1) \exp(-\gamma_1 d) - (\alpha + j\vartheta + c_S\gamma_2) \exp(-\gamma_2 d)\}. \quad (74)$$

More detailed evaluations of the above formulas should follow the pattern prescribed in Sections III and IV. They can be undertaken for the specific case when the need arises.

VI. VALIDITY OF THE THEORY

We have tried to make our results as generally applicable as possible. We have allowed for the presence of absorption in the various hologram gratings and for a slant of the fringe planes. But a whole range of assumptions had to be made to make the simple coupled wave analysis possible. It seems appropriate to recount these assumptions to make clear the region of validity of the coupled wave theory. We have assumed that:

(*i*) The electric field of the light is polarized perpendicular to the plane of incidence. However, the appendix gives an extension of the theory to allow also for light of parallel polarization.

(*ii*) A slant of the fringe planes with respect to the z-axis is allowed, except that these planes are perpendicular to the plane of incidence. (This is reflected in the assumption $\epsilon(x, z)$, $\sigma(x, z)$.) But this assumption is not made in the generalization which we have given in the appendix.

(*iii*) The spatial modulation of the refractive index and the absorption constant is sinusoidal.

(*iv*) There is a small absorption loss per wavelength and a slow energy interchange (per wavelength) between the two coupled waves. This condition is stated mathematically in equation (7) and justifies neglecting the second derivatives R'' and S'' in the analysis.

(*v*) There is the same average refractive index n for the regions inside and outside the grating boundaries. If the grating has interfaces with air, then Snell's law has to be used to correct for the angular changes resulting from refraction.

(*vi*) Light incidence is at or near the Bragg angle and only the diffraction orders which obey the Bragg condition at least approximately are retained in the analysis. The other diffraction orders are neglected.

A detailed mathematical justification of assumption *vi* is outside the scope of our simple analysis. One can advance physical arguments to show that this step limits the validity of the theory to "thick" gratings,

where the phase synchronism between the two coupled waves has enough time to develop a strong and dominating effect. Better definitions of a "thick grating" must come from more accurate theories which are available for special cases. A large amount of work has been done on acoustic diffraction gratings which correspond to the case of our unslanted, lossless, dielectric transmission-hologram gratings.[30] In acoustic diffraction one defines the parameter

$$Q = 2\pi\lambda d/n\Lambda^2 \tag{75}$$

as an appropriate measure of grating thickness. We can regard a grating as thick when the condition $Q \gg 1$ holds.[21,16] It appears that the coupled wave theory begins to give good results for values of $Q = 10$. This is particularly well demonstrated by Klein and his associates in theoretical and experimental work on acoustic gratings for the predictions of both the peak efficiencies and the angular sensitivities.[16,17,34] We hasten to add that for the majority of practical holograms the parameter Q is larger, and sometimes much larger, than 10.

Further checks of the validity of the coupled wave theory are provided by comparisons with accurate computer calculations and with experiments on special examples of gratings. Burckhardt has made computer calculations on unslanted, lossless, dielectric transmission holograms for selected values of grating parameters which are commonly encountered in holography.[18,19] Comparison with the results of the coupled wave theory shows very satisfactory agreement.[35] Measurements by Shankoff and Lin on dielectric transmission holograms prepared with dichromated gelatin yielded diffraction efficiencies approaching 100 percent, which agrees with the theory (even though there may be some uncertainty as to the exact nature of the refractive index variations).[10,11]

Efficiency measurements on thick absorption gratings for the case of transmission holograms were made by George, Mathews, and Latta.[36,37] Efficiencies approaching our predicted maximum value of 3.7 percent were observed.

Kiemle has studied unslanted ($\phi = 0$) reflection holograms for the special case of normal incidence ($\theta_0 = 0$) by analyzing equivalent four-terminal networks.[38] His treatment of absorption gratings corresponds to the material we discussed in Section 4.3 specialized to the case of $\theta_0 = 0$. But Kiemle's value of 2.8 percent for the maximum diffraction efficiency of absorptive reflection holograms does not agree with our prediction of 7.2 percent. This disagreement appears to derive from a set of restrictive assumptions made in Kiemle's work. Experimental observations on absorptive reflection holograms were made by

Lin and Lo Bianco.[9] Efficiency values as high as 3.8 percent were measured, which seems to support the predictions of the coupled wave theory. But further experiments are needed for a good confirmation.

VII. CONCLUSIONS

We have discussed a coupled-wave analysis of the Bragg diffraction of light by thick hologram gratings. This approach made it possible to derive simple algebraic formulas for the behavior of various types of holograms, even for the case of high diffraction efficiencies where the incident wave is strongly depleted. The treatment covers transmission holograms and reflection holograms, and it includes the spatial modulations of both the refractive index and the absorption constant. The influence of loss in the grating and of slanted fringes is also discussed. Formulas and their numerical evaluations are given for the diffraction efficiencies and the angular and wavelength sensitivities of various grating types.

For special cases we can compare the results of this theory with more accurate computations and with experimental observations. These comparisons give us the confidence to assume that the coupled wave predictions are good for a broad range of practical hologram types.

VIII. ACKNOWLEDGMENT

The author would like to acknowledge with thanks useful discussions with C. B. Burckhardt, and the patience of those who have waited so long for the promised completion of this article.

APPENDIX

Reduced Coupling for Light Polarized in the Plane of Incidence

In the body of this paper it was assumed that the incident light is polarized perpendicular to the plane of incidence. The purpose of this appendix is to show that we can use the results of the main paper also when the light is polarized in the plane of incidence, provided that we modify the coupling constant κ. Such a modification is suggested already by the dynamical theory of X-ray diffraction.

As in Section II we start with the wave equation

$$\nabla^2\mathbf{E} - \nabla(\nabla\cdot\mathbf{E}) + k^2\mathbf{E} = 0 \tag{76}$$

for the electric field in the grating. Here, in contrast to equation (1), we have described the field by the *vector* quantity $\mathbf{E}$ and have included

the term $\nabla(\nabla\cdot\mathbf{E})$, which is not necessarily zero. The constant k^2 is defined in equation (4). As in the main paper, we assume that only two waves are present in the grating, and put

$$\mathbf{E} = \mathbf{R}(z)e^{-j\boldsymbol{\varrho}\cdot\mathbf{x}} + \mathbf{S}(z)e^{-j\boldsymbol{\delta}\cdot\mathbf{x}} \tag{77}$$

using the vectors $\mathbf{R}$ and $\mathbf{S}$ to describe the amplitudes of the reference and signal waves. $\boldsymbol{\varrho}$ and $\boldsymbol{\delta}$ are the propagation vectors (as in Section II) which point in the direction of the wavenormals. They are related by equation (11). In addition we assume that, both, R and S are transverse waves, that is, that the following conditions hold

$$\begin{aligned}(\boldsymbol{\varrho}\cdot\mathbf{R}) &\equiv 0,\\ (\boldsymbol{\delta}\cdot\mathbf{S}) &\equiv 0.\end{aligned} \tag{78}$$

Combining equations (76), (77), and (78) we get, after separating terms with equal exponentials and neglecting second derivatives $\partial^2/\partial z^2$

$$-2j\rho_z\mathbf{R}' + j\varrho R_z' - 2j\alpha\beta\mathbf{R} + 2\kappa\beta\mathbf{S} = 0 \tag{79}$$

$$-2j\sigma_z\mathbf{S}' + j\delta S_z' + (\beta^2 - \sigma^2 - 2j\alpha\beta)\mathbf{S} + 2\kappa\beta\mathbf{R} = 0 \tag{80}$$

where R_z and S_z are the z-components of R and S, and the notation of Section II is used.

We now make the additional assumption that the polarizations of R and S do not change in the grating and write

$$\begin{aligned}\mathbf{R}(z) &= R(z)\mathbf{r},\\ \mathbf{S}(z) &= S(z)\mathbf{s},\end{aligned} \tag{81}$$

where $R(z)$ and $S(z)$ are the scalar amplitudes of the two waves, and $\mathbf{r}$ and $\mathbf{s}$ are polarization vectors independent of z. These vectors are normalized so that

$$(\mathbf{r}\cdot\mathbf{r}) = 1, \qquad (\mathbf{s}\cdot\mathbf{s}) = 1. \tag{82}$$

Because of (78) we have

$$(\mathbf{r}\cdot\boldsymbol{\varrho}) = 0, \qquad (\mathbf{s}\cdot\boldsymbol{\delta}) = 0. \tag{83}$$

After forming the dot products of $\mathbf{r}$ with eq. (79) and of $\mathbf{s}$ with (80) we use equations (81), (82), and (83) to arrive at

$$-2j\rho_z R' - 2j\alpha\beta R + 2\kappa\beta S(\mathbf{r}\cdot\mathbf{s}) = 0 \tag{84}$$

$$-2j\sigma_z S' + (\beta^2 - \sigma^2 - 2j\alpha\beta)S + 2\kappa\beta R(\mathbf{r}\cdot\mathbf{s}) = 0. \tag{85}$$

As in Section II, we introduce the abbreviations

$$c_R = \rho_z/\beta, \qquad c_S = \sigma_z/\beta, \tag{86}$$

and

$$\vartheta = (\beta^2 - \sigma^2)/2\beta, \tag{87}$$

which allow us to write the above equations in the form

$$c_R R' + \alpha R = -j\kappa(\mathbf{r}\cdot\mathbf{s})S \tag{88}$$

$$c_S S' + (\alpha + j\vartheta)S = -j\kappa(\mathbf{r}\cdot\mathbf{s})R. \tag{89}$$

These are coupled wave equations which govern the Bragg diffraction of light polarized parallel to the plane of incidence, and indeed, of light of arbitrary polarization. They are similar in form to the coupled wave equations (21) and (22) which were derived for perpendicular polarization. The only difference is a reduction of the effective coupling constant by the dot product $(\mathbf{r}\cdot\mathbf{s})$ of the two polarization vectors.

Referring to the grating geometry of Fig. 1 we have $(\mathbf{r}\cdot\mathbf{s}) = 1$ for light polarized perpendicular to the plane of incidence. For parallel polarization the value of this dot-product depends on the inclination angles, and we have a reduced effective coupling constant $\kappa_\parallel$ given by

$$\kappa_\parallel = \kappa(\mathbf{r}\cdot\mathbf{s}) = -\kappa\cos 2(\theta_0 - \phi). \tag{90}$$

We can apply the results of the main paper for parallel polarization if we replace κ by $\kappa_\parallel$. For this polarization there is the trivial case of a Bragg angle of 45° (that is, diffraction angles of 90°) where $(\mathbf{r}\cdot\mathbf{s}) = 0$ and the intensity of the diffracted light goes to zero.

REFERENCES

1. van Heerden, P. J., "Theory of Optical Information Storage in Solids," Appl. Opt., *2*, No. 4 (April 1963), pp. 393–400.
2. Smits, F. M., and Gallaher, L. E., "Design Considerations for a Semipermanent Optical Memory," B.S.T.J., *46*, No. 6 (July–August 1967), pp. 1267–1278.
3. Vitols, V. A., "Hologram Memory for Storing Digital Data," IBM Technical Disclosure Bull., *8*, No. 11 (April 1966), p. 1581.
4. Pennington, K. S., and Lin, L. H., "Multicolor Wavefront Reconstruction," Appl. Phys. Letters, *7*, (August 1965), pp. 56–57.
5. Denisyuk, Y. N., "On the Reproduction of the Optical Properties of an Object by the Wave Field of Its Scattered Radiation," Opt. Spectroscopy, *15*, No. 4 (October 1963), pp. 279–284.
6. Stroke, G. W., and Labeyrie, A. E., "White-light Reconstruction of Holographic Images Using the Lippman-Bragg Diffraction Effect," Phys. Letters, *20*, (March 1966), pp. 368–370.
7. Lin, L. H., Pennington, K. S., Stroke, G. W., and Labeyrie, A. E., "Multicolor Holographic Image Reconstruction with White-light Illumination," B.S.T.J., *45*, No. 4 (April 1966), pp. 659–660.

8. Upatnieks, J., Marks, J., and Fedorwicz, R., "Color Holograms for White Light Reconstruction," Appl. Phys. Letters, *8*, No. 11 (June 1966), pp. 286–287.
9. Lin, L. H., and Lo Bianco, C. V., "Experimental Techniques in Making Multicolor White Light Reconstructed Holograms," Appl. Opt., *6*, No. 7 (July 1967), pp. 1255–1258.
10. Shankoff, T., "Phase Holograms in Dichromated Gelatin," Appl. Opt., *7*, No. 10 (October 1968), pp. 2101–2105.
11. Lin L. H., "Hologram Formation in Hardened Dichromated Gelatin Films," Appl. Opt., *8*, No. 5 (May 1969), pp. 963–966.
12. Chen, F. S., LaMacchia, J. T., and Fraser, D. B., "Holographic Storage in Lithium Niobate," Appl. Phys. Letters, *12*, No. 7 (October 1968), pp. 223–224.
13. Close, D. H., Jacobson, A. D., Margerum, J. D., Brault, R. G., and McClumg, F. J., "Hologram Recording in Photopolymer Materials," Appl. Phys. Letters *14*, No. 5, (March 1969), pp. 159–160.
14. Leith, E. N., Kozma, A., Upatnieks, J., Marks, J., and Massey, N., "Holographic Data Storage in Three-Dimensional Media," Appl. Opt., *5*, No. 8 (August 1966), pp. 1303–1311.
15. Gabor, D., and Stroke, G. W., "The Theory of Deep Holograms," Proc. Royal Soc. of London, *A. 304*, (February 1968), pp. 275–289.
16. Klein, W. R., Tipnis, C. B., and Hiedemann, E. A., "Experimental Study of Fraunhofer Light Diffraction by Ultrasonic Beams of Moderately High Frequency at Oblique Incidence," J. Acoust. Soc. Amer., *38*, No. 2 (August 1965), pp. 229–233.
17. Klein, W. R., "Theoretical Efficiency of Bragg Devices," Proc. IEEE, *54*, No. 5 (May 1966), pp. 803–804.
18. Burckhardt, C. B., "Diffraction of a Plane Wave at a Sinusoidally Stratified Dielectric Grating," J. Opt. Soc. Amer., *56*, No. 11 (November 1966), pp. 1502–1509.
19. Burckhardt, C. B., "Efficiency of a Dielectric Grating," J. Opt. Soc. Amer., *57*, No. 5 (May 1967), pp. 601–603.
20. Bathia, A. B., and Noble, W. J., "Diffraction of Light by Ultrasonic Waves II," Proc. Royal Soc. of London, *220A*, (1953), pp. 369–385.
21. Phariseau, P., "On the Diffraction of Light by Progressive Supersonic Waves," Proc. Ind. Acad. Sci., *44A*, (1956), pp. 165–170.
22. Quate, C. F., Wilkinson, C. D., and Winslow, D. K., "Interaction of Light and Microwave Sound," Proc. IEEE, *53*, No. 10 (October 1965), pp. 1604–1623. This paper includes a comprehensive bibliography of work on acoustic scattering of light.
23. Gordon, E. I., and Cohen, M. G., "Electro-Optic Diffraction Grating for Light Beam Modulation and Diffraction," IEEE J. Quantum Elec., *QE-1*, No. 5 (August 1965), pp. 191–198.
24. Batterman, B., and Cole, H., "Dynamical Diffraction of X-Rays by Perfect Crystals," Rev. Mod. Phys. *36*, No. 3 (July 1964), pp. 681–717. This paper contains a review of the work on the diffraction of X-rays.
25. Saccocio, E. J., "Application of the Dynamical Theory of X-Ray Diffraction to Holography," J. Appl. Phys., *38*, No. 10 (September 1967), pp. 3994–3998.
26. Kogelnik, H., "Reconstructing Response and Efficiency of Hologram Gratings," Proc. Symp. Modern Optics, Polytechnic Inst., Brooklyn, March 1967, pp. 605–617.
27. Kogelnik, H., "Hologram Efficiency and Response," Microwaves, *6*, No. 11 (November 1967), pp. 68–73.
28. Born, M., and Wolf, E., *Principles of Optics*, New York: Pergamon Press, 1959, Chapter 12.
29. Bergstein, L., and Kermisch, D., "Image Storage and Reconstruction in Volume Holography," Proc. Symp. Mod. Opt., Polytechnic Inst. Brooklyn, March 1967, pp. 655–680.
30. Gordon, E. I., "A Review of Acoustooptical Deflection and Modulation Devices," Proc. IEEE, *54*, No. 10 (October 1966), pp. 1391–1401.
31. Belvaux, Y., "Influence of Emulsion Thickness and Absorption in Hologram Reconstruction," Physical Letters, *26A*, No. 5 (January 1968), pp. 190–191.
32. Nassenstein, H., "A New Hologram with Wavelength-Selective Reconstruction" Physical Letters, *28A*, No. 2 (November 1968), pp. 141–142.

33. Tien, P. K., unpublished work.
34. Klein, W. R., "Light Diffraction by Ultrasonic Beams of High Frequency Near Bragg Incidence," Proc. 5th Congress Int. D'Acoustique, Liege, D24 (September 1965).
35. Kogelnik, H., "Bragg Diffraction in Hologram Gratings with Multiple Internal Reflections," J. Opt. Soc. Amer., *57*, No. 3, (March 1967), pp. 431–433.
36. George, N., and Mathews, J. W., "Holographic Diffraction Gratings," Appl. Phys. Lett., *9*, No. 5 (September 1966), pp. 212–125.
37. Latta, J. N., "The Bleaching of Holographic Diffraction Gratings for Maximum Efficiency," Appl. Opt., *7*, No. 12 (December 1968), pp. 2409–2416.
38. Kiemle, H., "Lippman-Bragg Holograms as Periodic Ladder Networks," Frequenz, *22*, No. 7 (July 1968), pp. 206–211.